Asian Journal of Basic Science & Research
Volume 7, Issue 2, Pages 46-58, April-June 2025

Assessment of antimicrobial activity of 6-APA conjugated Zn coordination polymers

Denis A. Cabrera-Munguia[1], Sergio A. Vacio-Melendez[2], M. Ileana León-Campos[2], Eder I. Martínez-Mora[3], Claudia M. López-Badillo[4], Lucia F. Cano-Salazar[2], Tirso E. Flores-Guia[1], Francisco J. Enríquez-Medrano[5] & Jesús A. Claudio-Rizo[1*]

[1]Professor, [2]Student, [1,2]Materiales Avanzados, Facultad de Ciencias Químicas, Universidad Autónoma de Coahuila, Saltillo, Coahuila, México. [3]Química Orgánica, Facultad de Ciencias Químicas, Universidad Autónoma de Coahuila, Saltillo, Coahuila, México. [4]Materiales Cerámicos, Facultad de Ciencias Químicas, Universidad Autónoma de Coahuila, Saltillo, Coahuila, México. [5]Química Macromolecular y Nanomateriales, Centro de Investigación en Química Aplicada, Saltillo, Coahuila, México. Corresponding Author (Jesús A. Claudio-Rizo) Email: jclaudio@uadec.edu.mx[*]

DOI: http://doi.org/10.38177/AJBSR.2025.7206

Article Received: 03 April 2025 *Article Accepted: 08 June 2025* *Article Published: 14 June 2025*

ABSTRACT

Antimicrobial resistance is among the top ten global health threats. One way to overcome this problem is to design new antibiotics; with this aim, zinc (Zn) coordination polymers were synthesized by conjugation with 6-aminopenicilanic acid (6-APA) and benzene-1,3,5-tricarboxylic acid (BTC). The crystalline structure of Zn coordination polymers was analyzed by X-Ray Diffraction (XRD), the appropriate chemical coordination was studied by Attenuated Total Reflectance Fourier Transformed Infrared (ATR-FTIR), and their thermal stability was characterized by Thermogravimetric Analysis and Differential Thermal Analysis (TGA-DTA). The Zn coordination polymers were solubilized in water, obtaining different concentrations (25,000, 20,000, 15,000, 10,000, and 5,000 ppm (mg/L)) to emulate the concentration of commercial antibiotics. Then, these solutions were biologically characterized by testing the cell viability of human monocytes and porcine dermis fibroblasts, and a hemolysis assay to prove their biocompatibility. Their antimicrobial activity was tested against the *E. Coli* and *S. Aureus* strains in a liquid and solid medium (antibiograms). The results of ATR-FTIR indicated the suitable chemical coordination between Zn and its ligands, but the 6-APA loses its high crystallinity when it is conjugated with Zn; this effect is more evident when BTC is also added. However, the TGA-DTA analysis indicates that chemical conjugation increases the thermal stability of Zn conjugated polymers, especially when BTC is added in the synthesis process. The hemolysis test shows that Zn coordination polymers are slightly cytotoxic, but the cell viability assays indicate that 6-APA Zn conjugated polymers exhibits the highest cell viability and thus better biocompatibility. However, when the antimicrobial properties of Zn coordination polymers were tested, the ligand 6-APA shows the highest bactericidal properties in liquid and solid medium for both *E. Coli* and *S. Aureus* strains.

Keywords: 6-APA; Zn; BTC; Coordination Polymers; *E. Coli*; *S. Aureus*; Bactericidal Properties; Antimicrobial Resistance; Hemolysis.

1. Introduction

Nowadays, antimicrobial resistance (AMR) is a challenge for public health and contemporary medicine, since it represents a threat to human beings due to the increase in health care costs and mortality; it is estimated that the deaths from AMR will increase to up to 10 million per year by 2050 [1]. Some factors that accelerated the AMR phenomenon are the misuse and abuse of antimicrobial agents in agriculture, veterinary, and human health over the decades, as well as poor infection control practice, inadequate sanitation, and improper food handling [1,2,3]. A high content of biocides and antibiotics polluted the air, water, and soil, generating genetic change in bacteria, viruses, fungi, and parasite populations, which allows them to survive and grow even in the presence of antimicrobial agents designed to kill them [1,2].

In the specific case of bacteria, the most common mechanism to evade antimicrobial drugs are inhibition of drug binding sites, reduce the antibiotic intracellular concentration, enzymes that modify or degrade antibiotics, reduction of the membrane's permeability and biofilms formation that avoids antibiotic penetration and enhance the resistance [1,4,5]. Among the bacterial strains able to escape from the bactericidal effect of antibiotics are pathogens groups under the acronym ESKAPE: Enterococcus faecium, Staphylococcus aureus, Klebsiella pneumoniae, *Acinetobacter baumannii*, *Pseudomonas aeruginosa*, and *Enterobacter* species [6,7].

On the other hand, 6-APA is penicillin's core structure, consisting of a fused beta-lactam and a thiazolidine ring. The discovery of 6-APA in 1957 by the scientist in the Beecham Research Laboratories was a watershed in the fight

against infection at that time, and in the significant advances in the development of beta-lactam antibiotics. These latter are the most active groups against bacteria that have stood the test of time, except for cefaloridine and methicillin [8].

The bactericidal mechanism of beta-lactam antibiotics is the inhibition of the bacterial cell walls, leading to the lysis and death of the bacteria. However, the resistance mechanism comprises participation by the enzymes β-lactamases that hydrolyse the β-lactam ring from antibiotics, rendering it inactive, which is why the β-lactam ring is often modified with a variable side chain to overcome the antimicrobial resistance mechanism [9,10].

In addition, metal ions like silver (Ag), gold (Au), cobalt (Co), copper (Cu) and zinc (Zn) have been proved to present bactericidal properties [11,12], where the typical action mechanism is the release of toxic metal ions and formation of reactive oxygen species (ROS) [11,13]. The low cost of Zn and its high ability to form coordination polymers make it an excellent option for coordinating polymers assembled with carboxylic acid ligands such as benzene-1,4-dicarboxylic acid (BDC) or benzene-1,3,5-tricarboxylic acid (BTC) [11,13,14].

Thus, this research aims to synthesize Zn coordination polymers conjugated to 6-APA and BTC at room temperature using water as a solvent. The crystalline structure, chemical conjugation, and thermal stability were analyzed by XRD, ATR-FTIR, and TGA-DTA, respectively. Also, their biocompatibility was analyzed with the hemolysis test and cell viability of human monocytes and porcine dermis fibroblasts. However, the main goal is to assess their bactericidal properties against *E. Coli* and *S. Aureus*, comparing their performance with 6-APA in liquid and solid medium by agar diffusion test.

1.1. Study objectives

1) Synthesis of coordination polymers based on zinc, 6-APA and BTC.

2) Characterization of the zinc coordination polymers to evaluate the chemical coordination, crystallinity and thermal stability.

3) To evaluate the biocompatibility of the zinc coordination polymers by hemolysis and 3-(4,5-dimethylthiazol-2-yl)-2,5-diphenyltetrazolium bromide (MTT) test.

4) To assess the bactericidal properties of zinc coordination polymers under liquid and solid medium.

5) To use ANOVA to evaluate the effect of time, concentration, and type of zinc coordination polymers on the bactericidal activity against *S. Aureus* and *E. Coli*.

2. Materials and Methods

2.1. Synthesis of Zn coordination polymers

In a typical procedure, 17.71 mmol of $Zn(NO_3)_2.6H_2O$ (≥99%) was dissolved in 25 mL of deionized water, and 14.45 mmol of 6-APA was separately diluted in 25 mL of deionized water. Both solutions are mixed and maintained under stirring for 24 h at room temperature. Later, the solution is filtered and washed with deionized water until the pH is 7. The yellowish precipitate is dried at 60ºC overnight. The Zn coordination polymer is called ZA, which is crushed and stored until use.

The other Zn coordination polymer synthesis requires the dissolution of 17.71 mmol of $Zn(NO_3)_2.6H_2O$ in 15 mL of deionized water, by separately diluting 14.45 mmol of 6-APA in 20 mL of deionized water, and another solution of 15.22 mmol of BTC in 15 mL of ethanol. The solutions of 6-APA and BDC were mixed, and then, the zinc solution was added. The final solution was kept under stirring for 24 h at room temperature. Then, the solution is filtered and washed with deionized water until the pH is 7. The white precipitate is dried at 60ºC overnight. The Zn coordination polymer is called ZAT, which is crushed and stored until use.

2.2. Physicochemical characterization of Zn coordination polymers

The XRD diffractograms of 6-APA, ZA, and ZAT were acquired in a 2θ range from 7º to 80º with a Cu Kαx ray source (λ=1.540 Å) using a *SAXS-Emc2, Anton Paar* diffractometer. The infrared spectra of 6-APA and the Zn conjugated polymers were acquired with a resolution of 16 cm^{-1} from 4000 to 600 cm^{-1} using *Perkin Elmer Frontier* equipment. For the thermogravimetric analysis (TGA), it was used a *TGA-4000 Perkin Elmer* thermal analyzer was used, where 5 mg of sample was heated from room temperature until 800ºC with a heating rate of 20ºC/min, and an N_2 flow of 20 mL/min as inert atmosphere

2.3. Hemolysis test

The hemolysis test measures the hemoglobin released when the red blood cell membrane is destroyed. A human blood sample was centrifuged at 3000 rpm for 5 min, the plasma was decanted, and the erythrocytes were obtained. Red blood cells were washed with 5 ml of Alsever's solution. Then, in Eppendorf tubes, triplicate samples of 112 µL of purified erythrocytes were taken and diluted in 1348 µL of Alsever's solution along with 100 µL of the sample solution at 25000, 20000, 15000, 10000, and 5000 ppm (mg/L). The Eppendorf tubes were incubated under static conditions at 37ºC for 1 h. Then, 200 µL of this solution was added to each well of a 96-microplate. The hemolytic capacity (%) of Zn coordination polymers was calculated by the ratio of the absorbance value at 415 nm obtained for coordination polymers to the absorbance values of positive control (water) and negative control (Alsever's solution), using a MultiSkan Sky, Thermo Scientific spectrophotometer. The hemolysis percentage was determined by equation (1) [15].

$$Hemolysis, \% = \frac{sample\ absorbance - control(-)\ absorbance}{control(+)\ absorbance - control(-)\ absorbance} \quad (1)$$

2.4. Cell viability test

The variation of the metabolism of porcine dermis fibroblasts and human monocytes growing on every solution of Zn coordinate polymers at different concentrations was assessed. In each well of a 96-microplate, 100 µL of cell suspension in DMEM culture medium and 100 µL of the sample solution were added. As a control, each well was filled with 100 µL of Phosphate Buffer Solution 1 X (PBS 1 X sterilized) instead of the sample solution. The 96-microplate was incubated for 24 and 48 h at 37ºC. Then, 10 µL of MTT (1 wt.%) was added to each well, and afterwards the cells were incubated under culture conditions for 3 h at 37 °C. At that point, the medium was tapped, and the absorbance of the solutions was estimated at 560 nm using a MultiSkan Sky, Thermo Scientific spectrophotometer. The absorbance of formazan generated by cells growing in wells without Zn coordination

polymers is equal to 100% of viability (control); thus, the cell viability percentage was calculated using equation (2) [16].

$$Cell\ viability, \% = \frac{Absorbance\ of\ Zn\ coordination\ polymer\ solution}{control\ absorbance} \quad (2)$$

2.5. Bactericidal properties in liquid medium

Suspensions of *E. Coli* and *S. Aureus* in Eosin Methylene Blue Agar (EMB) and Tryptone Glucose extract agar (TG), respectively, as a culture medium, were added 100µL to the lls of a 96-microplate and 100 µL of the sample solution at 25000, 20000, 15000, 10000, and 5000 ppm. Instead of 100 µL of the sample, 100 µL of gentamicin at 20 ppm was used as a control. The 96-microplate was incubated at 37ºC for 24 and 48 h. The absorbance of the solutions was estimated at 600 nm, using a MultiSkan Sky, Thermo Scientific spectrophotometer. The inhibition percentage was calculated using equation (3).

$$Inhibition, \% = \frac{Absorbance\ of\ Zn\ coordination\ polymer\ solution}{control\ absorbance} \quad (3)$$

2.6. Bactericidal properties in solid medium by agar diffusion test

In-vitro bacterial inhibition tests were performed using EMB and TG as a culture medium for *E. Coli* and *S. Aureus*, respectively. The agar was prepared by dissolving 36 g of EMB or 24 g of TG in 1 liter of distilled water and was heated until dissolved. The culture medium was sterilized at 124ºC for 15 min. Once the medium was ready, it was poured into Petri dishes, which were previously sterilized. Filter paper disks of around 1 cm^2 were wet with 10 µL of the coordination polymer solution at different concentrations. The disks were placed in the center of the culture medium dishes, to measure the inhibition halo. The disks were wet with 10 µL of Gentamicin prepared at 20 ppm, which was used as a control. The bacterial strain (*E. Coli* or *S. Aureus*) was seeded homogeneously in the Petri dishes, including problem samples and controls, using a sterile loop. The bacterium was incubated for 24 h at 37ºC to measure its growth in the presence of the disks impregnated with the Zn coordination polymers. The inhibition capacity of *E. coli* and *S. Aureus* was calculated by comparing the diameter of the halo formed by the disk with the diameter generated by the positive control. The equation (4) was applied to estimate the inhibition growth percentage [15].

$$Growth\ inhibition, \% = \frac{Composite\ diameter}{Control\ diameter} x100 \quad (4)$$

3. Results and Discussion

3.1. Physicochemical characterization

Figure 1 shows the XRD patterns of 6-APA, ZA, and ZAT coordination polymers. The powder of 6-APA indicates the main diffraction signals at 2θ = 10.6º, 12.2º, 16.6º, 17.7º, 24.3º, and 31.5º. The prominent diffraction peaks for ZA at 2θ = 9.3º (0 1 1) and 11.6º(0 0 2), which are the characteristics diffraction peaks and crystal planes of Zn-MOF [17], however, additional peaks at 12.3º and 31.3º indicated that coordinated polymerization was not concluded under the synthesis conditions, since similar peaks are found in pure 6-APA, as well as the low intensity of ZA, which is twenty times lower than 6-APA. This result is related to the chirality of the 6-APA molecule.

The diffraction pattern of ZAT includes 6-APA and BTC, both of which are used as organic linkers. It is observed that a sample with a higher crystallinity than ZA but is more amorphous than 6-APA, which again implies the low coordinated polymerization between Zn and both linkers. The main diffraction signals of ZAT at 7.5º (0 1 1), 13º (0 2 0) and 13.3º(1 0 2) correspond to the monoclinic crystalline structure of Ni-BTC [18] instead of a cubic space group of Zn-BTC [19], which is attributed to the steric effect between both linkers and zinc.

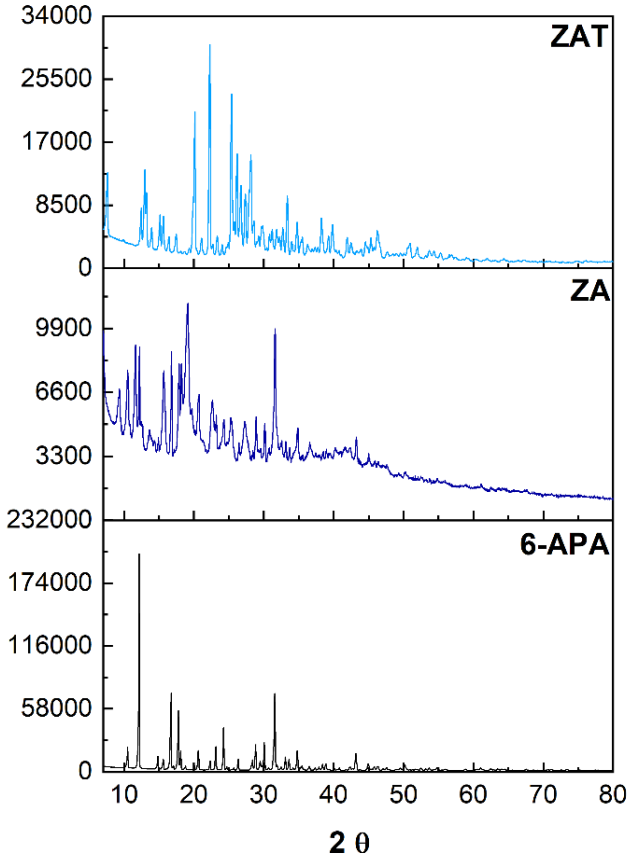

Figure 1. Diffractograms of 6-APA, ZA and ZAT

Figure 2 exhibits the ATR-FTIR spectra of 6-APA, ZA, and ZAT samples. The spectrum of 6-APA shows the typical vibration for the beta-lactam ring's carbonyl group (C=O), which is observed at 1770 cm^{-1}. The band at 1530 cm^{-1} corresponds to the bending vibration of the amide group (N-H). The C-O stretching vibration is assigned to the 1335 cm^{-1} and 1381 cm^{-1} values. The band at around 3200 cm^{-1} is related to hydroxyl(-OH) and amine (-NH-) vibrations. Also, C-H stretching frequencies appear in the range 3100-3000 cm^{-1}, the C-H in-plane bending vibrations in the range 1300-1000 cm^{-1}, and C-H out-of-plane bending vibrations in the range 1000-750 cm^{-1}. While the broadband within the range of 2250-2750 cm^{-1} indicates the presence of intermolecular hydrogen bonding due to carboxylic OH groups [20,21].

The FTIR spectrum of ZA shows the band characteristic of the carboxylic groups beta-lactam ring with a slight displacement to 1735 cm^{-1} and with very low intensity in comparison with the precursor 6-APA. In addition, the band at 1530 cm^{-1} related to the amide group and the broadband within the 2250-2750 cm^{-1} range disappeared. This suggests that coordination with Zn is mediated by coordination with the carboxylic and amide groups of the beta-lactam ring. In comparison, the FTIR spectrum of ZAT shows a broad band within the range of 3600-3200

cm^{-1} that belongs to the stretching vibrations of hydroxyl groups due to the presence of BTC linker. Similarly, it is observed at 1710 cm^{-1} and a broad band with a maximum at 1180 cm^{-1} related to the stretching vibration of C=O and C-O. In addition, the band at 1530 cm^{-1} and the broadband within the range of 2250-2750 cm^{-1} appears again. This result is in line with the XRD results where both linkers compete with each other to be coordinated with Zn ions due to a steric effect [22]. Unfortunately, due to the spectral range, the absorption peak at 575.9 cm^{-1} corresponding to Zn-O stretching vibration cannot be observed.

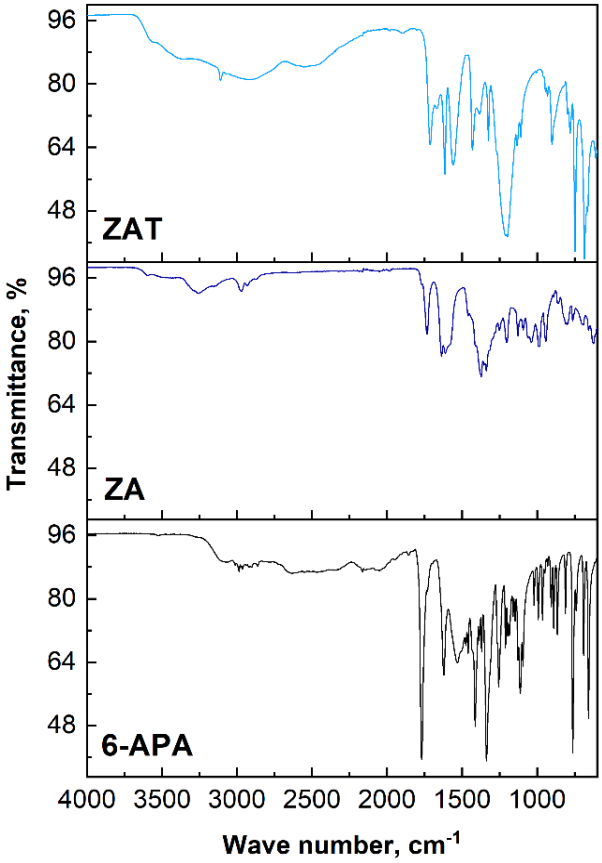

Figure 2. ATR-FTIR spectra of 6-APA, ZA and ZAT

Figure 3 presents simultaneously the TGA-DTA curves of 6-APA, ZA, and ZAT samples. The first weight loss for 6-APA material is around 194ºC (40%), which is attributed to the breakdown of the beta-lactam ring, as previously reported [23].

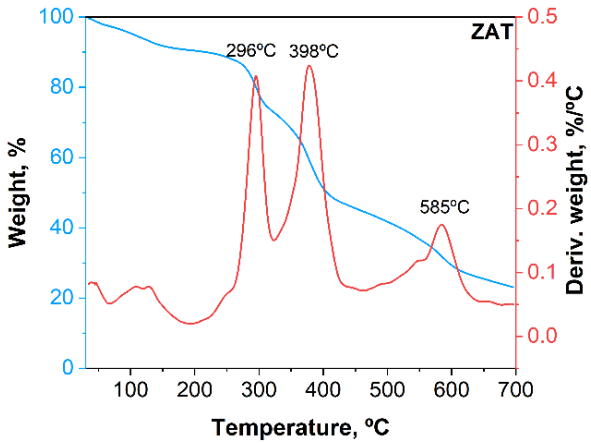

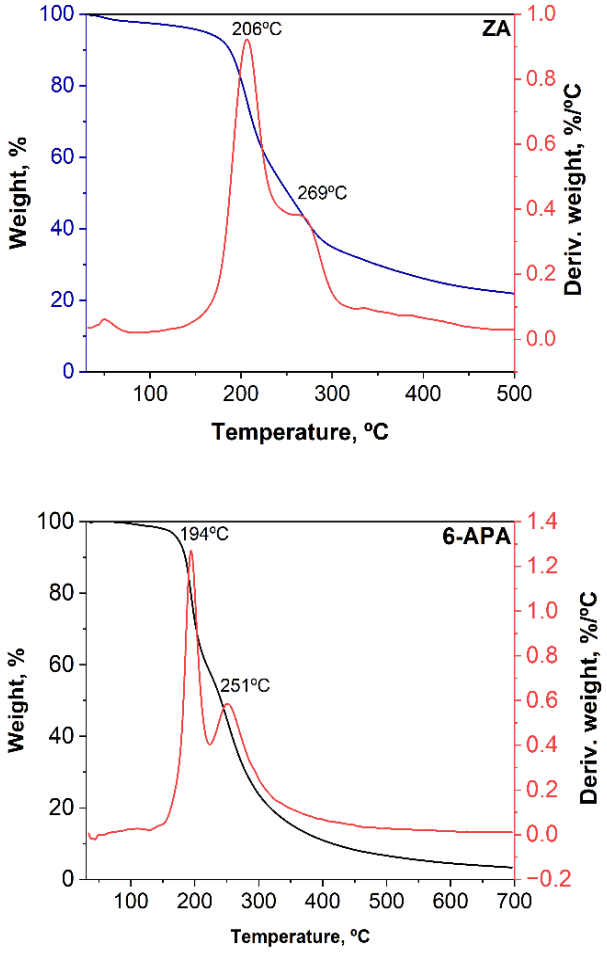

Figure 3. TGA-DTA of a) 6-APA, b) ZA and c) ZAT

The second weight loss is attributed to the organic matter decomposition to ashes, leading to a mass residue of only 3.3%. The coordination between zinc and 6-APA presents the same type of weight loss; however, incorporating zinc leads to a significant thermal resistance, increasing the temperature between 12 and 18ºC, obtaining a residual mass of 20.1% due to the presence of ZnO. In the case of the ZAT sample, the addition of BTC gives rise to a third peak and a more stable compound. At temperatures lower than 200ºC, small peaks are related to the mass loss of water(10 %) due to the dihydroxylation of carboxylic groups found mainly in the BTC ligand. Then, the first mass loss at 296ºC is related to the degradation of the beta-lactam ring, losing around 15%. The second peak at 378ºC with a mass loss of 27.8% is associated with the decarboxylation of BTC. The third mass loss at 585ºC belongs to benzene ring decomposition, leading to a residual mass of 23.1%.

3.2. Biocompatibility characterization

The hemolysis assay is an *in vitro* test that analyzes the damage that a chemical compound can make to erythrocytes, resulting in hemoglobin in the surroundings, and is a method to evaluate the biocompatibility and possible toxicity of a substance[24]. In this case, the hemolysis test analyzes the disintegration of erythrocytes when they are in contact with water solutions of 6-APA, ZA, and ZAT. Figure 4 indicates that all samples demonstrated a hemolysis percentage lower than 5% but higher than 0% demonstrating a slightly hemolytic character. However, materials with a hemolysis percentage lower than 5% are considered biocompatible [16].

Asian Journal of Basic Science & Research
Volume 7, Issue 2, Pages 46-58, April-June 2025

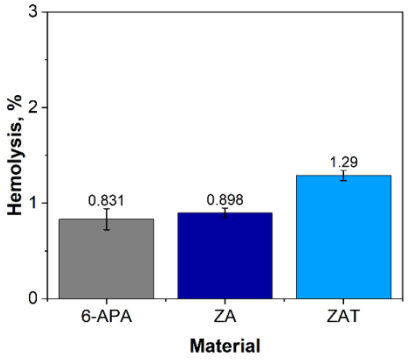

Figure 4. Hemolysis percentage of 6-APA, ZA and ZAT

Fibroblasts are cells present in all tissues. Some of their functions are the production of collagen and elastin and the regulation of the extracellular matrix. Additional functions are the recognition of pathogens, inducing the recruitment of inflammatory cells via cytokines and growth factors, and also releasing antimicrobial peptides [26]. Then, it is relevant to analyze its cell viability in the presence of Zn-coordinated polymers and evaluate the biocompatibility of these new compounds. The results (Figure 5 (left)) suggest that all samples exhibit values higher than 60% except for ZAT after 48 h of exposure. A three-way ANOVA (Analysis of Variance) was applied to experimental data using MINITAB 18 with a confidence level of 95%, indicating that in general, the time does not affect the cell viability of fibroblasts. In this case, the fibroblasts' biocompatibility is ZA>ZAT>6-APA, but also a concentration of 25,000 ppm is the best to obtain a higher cell viability.

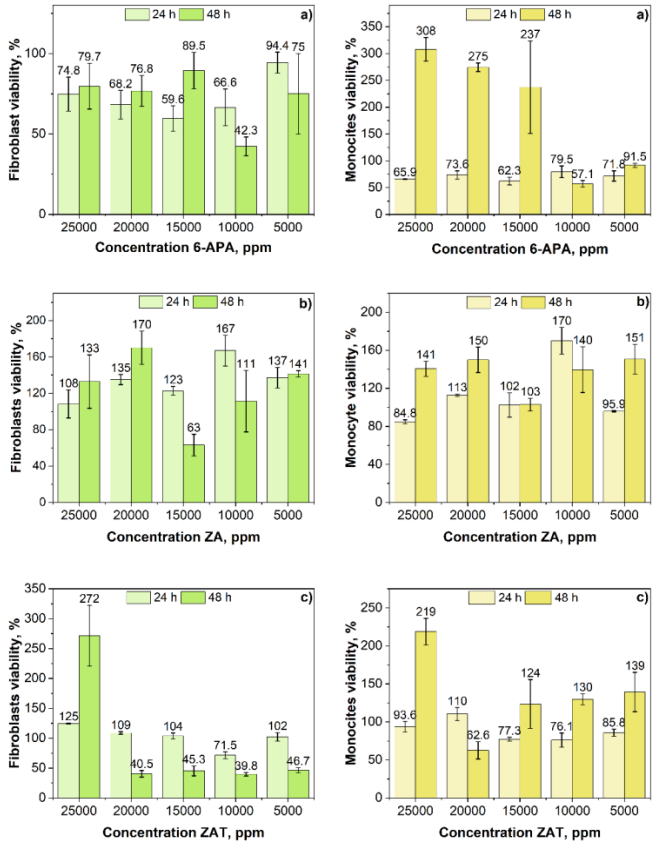

Figure 5. Porcine dermis fibroblast (left) and human monocytes (right) cell viability of a) 6-APA, b) ZA and c) ZAT

Monocytes are leukocytes of the innate immune system whose primary role is protecting the host from pathogens by promoting disease regression or allowing disease progression. They can also be differentiated into macrophages and/or dendritic cells [27]. Studying its viability in the presence of these new coordination polymers is also helpful. The results (Figure 5 (right)) with cell viability higher than 60% indicate that the mitochondrial function of these cells is not affected in the presence of a water solution of Zn-coordinated polymers [16]. A three-way ANOVA was done using MINITAB 18 with a confidence level of 95%. In general terms, it is observed that a higher monocyte viability after 48 h, the viability percentage of 6-APA is statistically equal to ZA compound, where the ZAT polymer shows the lowest cell viability values. In the same way, the highest cell viability for all samples is obtained with the highest concentration of 25000 ppm, confirming that Zn coordination polymers are biocompatible.

3.3. Antimicrobial activity

First, the antimicrobial activity of Zn-coordinated polymers was analyzed in liquid medium, which differentiated from the solid media in how the bactericidal activity is determined. In liquid media, the inhibition is typically measured by the absence of turbidity, demonstrating that microorganisms are not growing. While in solid media, inhibition is visualized as a clear zone around the antimicrobial agent (inhibition halo) [28].

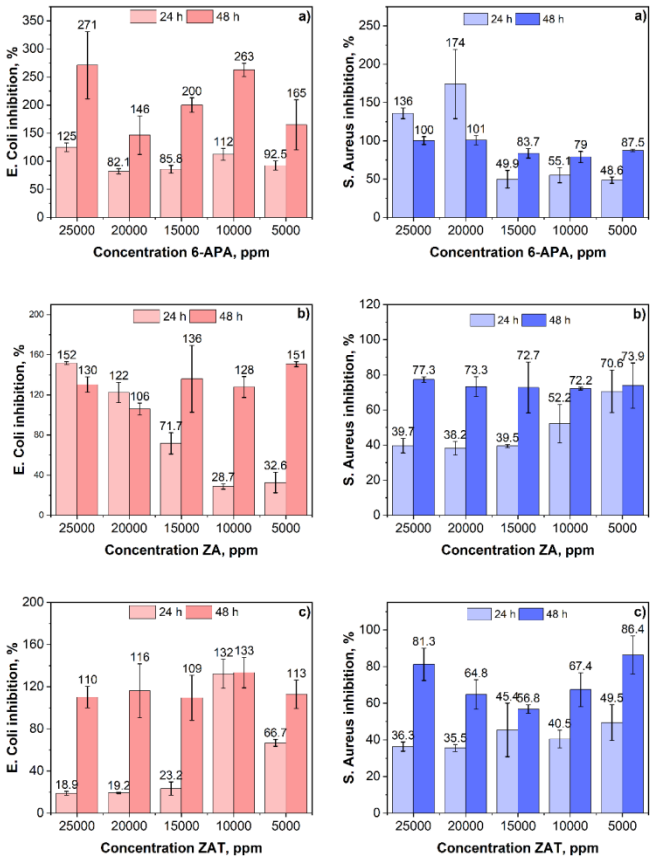

Figure 6. *E. Coli* (left) and *S. Aureus* (right) antimicrobial inhibition in liquid media of a) 6-APA, b) ZA and c) ZAT

The experimental data (Figure 6) were analyzed again with a three-way ANOVA for *E. Coli*(left) and *S. Aureus*(right) obtaining the same pattern in both bacteria strains. The antimicrobial activity is increased when the time reaches 48 h of exposure, the concentration has no effect on the bacterial inhibition, so it is preferable to use the

lower concentration of 5,000 ppm. In addition, 6-APA shows the highest antimicrobial inhibition in both *E. Coli* and *S. Aureus*, and statistically, ZA and ZAT showed the same bactericidal activity.

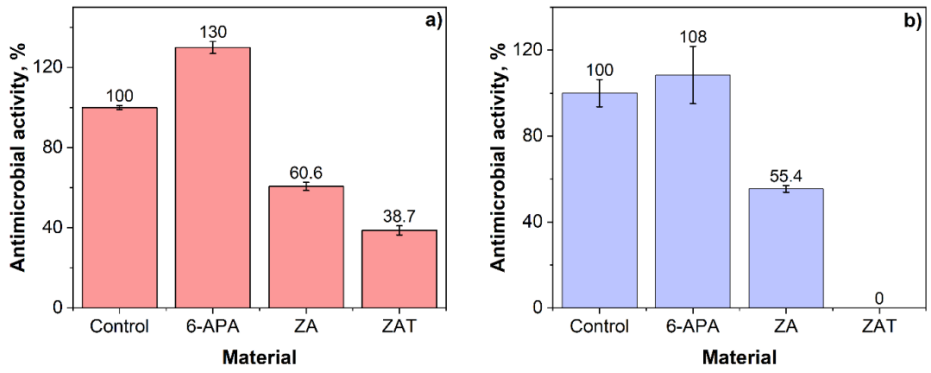

Figure 7. a) *E. Coli* and b) *S. Aureus* antimicrobial inhibition in solid media of Zn coordination polymers

Figure 7 presents the bactericidal activity in solid media of 6-APA, ZA and ZAT coordination polymers in *E. Coli* (Figure 7a)) and *S. Aureus* (Figure 7b)). In the case of *E. Coli* the Tukey probe with a confidence level of 95% can be state that 6-APA solution present a higher bactericidal property than the control (gentamicin). However, in *S. Aureus*, the Tukey probe with a confidence level of 95% can be used to state that the control (gentamicin) and 6-APA solution present the same bactericidal properties. The two bacterial strains differ due to their cell wall structure. Thus, *E. Coli* (Gram positive) with a thinner peptidoglycan layer than *S. Aureus* (Gram negative) is more susceptible to the attack of the beta-lactam ring. The high bactericidal activity of 6-APA in comparison to ZA and ZAT is related to the lack of accessibility of the beta-lactam ring to the bacterial cell wall after coordinated polymerization as well as the crystallinity loss of 6-APA, since crystals can also cause physical damage to the bacterial cell wall.

4. Conclusions

The XRD and ATR-FTIR indicated the suitable synthesis of Zn coordination polymers conjugated to 6-APA and BTC. However, the chemical conjugation leads to coordination polymers ZA and ZAT with a crystallinity twenty times and seven times lower than 6-APA, respectively. This is due to the high chirality of the 6-APA molecule, which prevents chain polymerization and thus the obtention of more amorphous materials. Nonetheless, the conjugation of Zn with 6-APA increased the thermal stability of 6-APA. This effect is more remarked when BDC is added as an additional ligand.

The hemolysis test indicates that 6-APA Zn conjugated polymers show a slightly cytotoxic effect on erythrocytes, especially when BTC is added. However, the cell viability assays of porcine dermis fibroblasts and human monocytes indicate that the most biocompatible coordination polymer is ZA even after 48 h. However, the antimicrobial properties in liquid and solid medium for Zn coordination polymers were very low with respect to 6-APA, which is attributed to the loss of the β-lactam ring to access the bacterial cell wall after polymer coordination.

The hemolysis test shows that Zn coordination polymers are slightly cytotoxic, but the cell viability assays indicate that ZA conjugated polymer exhibit the highest cell viability and thus better biocompatibility. However, when the

antimicrobial properties of Zn coordination polymers were tested, the ligand 6-APA showed the highest bactericidal properties in liquid and solid medium for both *E. Coli* and *S. Aureus* strains.

5. Future Recommendations

Future research suggestions include:

1) The use of other biocompatible element, such as Ag, Ca, Zr, Ti or Fe.

2) The application of other antibiotic precursor such as 7-aminocephalosporanic acid (7-ACA).

3) To use hydrothermal synthesis to ensure the suitable coordinated polymerization.

4) To include SEM (Scanning Electron Microscope) micrographs analysis to evaluate the crystal size and form.

5) To include other bacteria strains such as *P. Aeruginosa.*

6) To synthesize coordination polymers that preserve the crystalline structure of the antibiotic precursor and damage the bacterial cell membrane.

Declarations

Source of Funding

This study did not receive any grant from funding agencies in the public or not-for-profit sectors.

Competing Interests Statement

The authors declare that they have no conflict of interest.

Consent for publication

The authors declare that they consented to the publication of this study.

Authors' contributions

All the authors took part in literature review, analysis, and manuscript writing equally.

Informed Consent

Not applicable.

References

[1] Oliveira, M., Antunes, W., Mota, S., et al. (2024). An Overview of the Recent Advances in Antimicrobial Resistance. Microorganisms, 12(9): 1920. https://doi.org/10.3390/microorganisms12091920.

[2] Salam, M.A., Al-Amin, M.Y., Salam, M.T., et al. (2023). Antimicrobial Resistance: A Growing Serious Threat for Global Public Health. Healthcare (Switzerland), 11(13): 1946. https://doi.org/10.3390/healthcare11131946.

[3] Sharma, S., Chauhan, A., Ranjan, A., et al. (2024). Emerging challenges in antimicrobial resistance: implications for pathogenic microorganisms, novel antibiotics, and their impact on sustainability. Front Microbiol., 15: 1403168. https://doi.org/10.3389/fmicb.2024.1403168.

[4] Ahmed, S.K., Hussein, S., Qurbani, K., et al. (2024). Antimicrobial resistance: Impacts, challenges, and future prospects. J Med Surg Public Health, 2: 100081. https://doi.org/10.1016/j.glmedi.2024.100081.

[5] Irfan, M., Almotiri, A., & AlZeyadi, Z.A. (2022). Antimicrobial Resistance and Its Drivers—A Review. Antibiotics, 11(10): 1362. https://doi.org/10.3390/antibiotics11101362.

[6] Reygaert, W.C. (2018). An overview of the antimicrobial resistance mechanisms of bacteria. AIMS Microbiol., 4: 482–501. https://doi.org/10.3934/microbiol.2018.3.482.

[7] Mancuso, G., Midiri, A., Gerace, E., & Biondo, C. (2021). Bacterial antibiotic resistance: the most critical pathogens. Pathogens, 10(10): 1310. https://doi.org/10.3390/pathogens10101310.

[8] Rolinson, G.N., & Geddes, A.M. (2007). The 50th anniversary of the discovery of 6-aminopenicillanic acid (6-APA). Int J Antimicrob Agents, 29(1): 3–8. https://doi.org/10.1016/j.ijantimicag.2006.09.003.

[9] Zango, U.U., Munir, I., Abubakar Shawai, S.A., & Shamsuddin, I.M. (2019). A review on β-lactam antibiotic drug resistance. MOJ Drug Des Develop Ther., 3(2): 52–58. https://doi.org/10.15406/mojddt.2019.03.00080.

[10] Kim, D., Kim, S., Kwon, Y., et al. (2023). Structural Insights for β-Lactam Antibiotics. Biomol Ther (Seoul), 31: 141–147. https://doi.org/10.4062/biomolther.2023.008.

[11] Colinas, I.R., Rojas-Andrade, M.D., Chakraborty, I., & Oliver, S.R.J. (2018). Two structurally diverse Zn-based coordination polymers with excellent antibacterial activity. CrystEngComm., 20: 3353–3362. https://doi.org/10.1039/c8ce00394g.

[12] Wang, D., Xing, X., Ye, X., et al. (2019). Synthesis, characterization and antibacterial activity of Zn(II) coordination polymer. J Inorg Biochem., 194: 153–159. https://doi.org/10.1016/j.jinorgbio.2019.02.014.

[13] Yuan, K., Ye, X., Liu, W., et al. (2021). Preparation, characterization and antibacterial activity of a novel Zn(II) coordination polymer derived from carboxylic acid. J Mol Struct., 1241: 130624. https://doi.org/10.1016/j.molstruc.2021.130624.

[14] Nakhaei, M., Akhbari, K., Kalati, M., & Phuruangrat, A. (2021). Antibacterial activity of three zinc-terephthalate MOFs and its relation to their structural features. Inorg Chim Acta, 522: 120353. https://doi.org/10.1016/j.ica.2021.120353.

[15] Cabrera-Munguia, D.A., Claudio-Rizo, J.A., Becerra-Rodríguez, J.J., et al. (2023). Enhanced biocompatibility and bactericidal properties of hydrogels based on collagen-polyurethane-aluminium MOFs for biomedical applications. Bull Mater Sci., 46: 100. https://doi.org/10.1007/s12034-023-02930-6.

[16] Cabrera-Munguia, D.A., León-Campos, M.I., Claudio-Rizo, J.A. et al. (2021). Potential biomedical application of a new MOF based on a derived PET: synthesis and characterization. Bull Mater Sci., 44: 245. https://doi.org/10.1007/s12034-021-02537-9.

[17] Liu, Z., Bakhtari, M.F., & Han, X. (2024). Preparation of bimetallic Pb/Zn metal-organic framework @graphene oxide composite and its adsorption performance for Pb(II) and Zn(II). Environ Eng Res., 29: 240198. https://doi.org/10.4491/eer.2024.198.

[18] Yaqoob, L., Noor, T., Iqbal, N., et al. (2019). Development of nickel-BTC-MOF-derived nanocomposites with rGO towards electrocatalytic oxidation of methanol and its product analysis. Catalysts, 9(10): 856. https://doi.org/10.3390/catal9100856.

[19] Sarkar, A., Adhikary, A., Mandal, A., et al. (2020). Zn-BTC MOF as an Adsorbent for Iodine Uptake and Organic Dye Degradation. Cryst Growth Des., 20: 7833–7839. https://doi.org/10.1021/acs.cgd.0c01015.

[20] Güngör, Ö.Ö.N., Gürkan, P., Özçelik, B., & Oyardi, Ö. (2016). Synthesis and antimicrobial activities of new higher amino acid Schiff base derivatives of 6-aminopenicillanic acid and 7-aminocephalosporanic acid. J Mol Struct., 1106: 181–191. https://doi.org/10.1016/j.molstruc.2015.10.074.

[21] Swaminathan, J., Ramalingam, M., Sethuraman, V., et al. (2010). FT-IR, FT-Raman, ab initio and DFT structural and vibrational frequency analysis of 6-aminopenicillanic acid. Spectrochim Acta A Mol Biomol Spectrosc., 75: 183–190. https://doi.org/10.1016/j.saa.2009.10.010.

[22] Phuong, N.T., Buess-Herman, C., Thom, N.T., et al. (2016). Synthesis of Cu-BTC, from Cu and benzene-1, 3,5-tricarboxylic acid (H3BTC), by a green electrochemical method. Green Process Synth., 5: 537–547. https://doi.org/10.1515/gps-2016-0096.

[23] Su, M., Sun, H., Zhao, Y., et al. (2016). Degradation Kinetics and Mechanism of a β-Lactam Antibiotic Intermediate, 6-Aminopenicillanic Acid, in a New Integrated Production Process. J Pharm Sci., 105: 139–146. https://doi.org/10.1016/j.xphs.2015.11.026.

[24] Liang, Y., Zhao, X., Hu, T., et al. (2019). Adhesive Hemostatic Conducting Injectable Composite Hydrogels with Sustained Drug Release and Photothermal Antibacterial Activity to Promote Full-Thickness Skin Regeneration During Wound Healing. Small, 15: 1900046. https://doi.org/https://doi.org/10.1002/smll.201900046.

[25] Cabrera-Munguia, D.A., Castañeda-Calzoncit, C.E., Claudio-Rizo, J.A., et al. (2025). In vitro biocompatibility and drug release of collagen-mo-complexes hydrogels for tissue engineering. Macromol Res. https://doi.org/10.1007/s13233-025-00375-w.

[26] Bautista-Hernández, L.A., Gómez-Olivares, J.L., Buentello-Volante, B., & Bautista-de Lucio, V.M. (2017). Fibroblasts: the unknown sentinels eliciting immune responses against microorganisms. Eur J Microbiol Immunol. (Bp), 7: 151–157. https://doi.org/10.1556/1886.2017.00009.

[27] Karlmark, K., Tacke, F., & Dunay, I. (2012). Monocytes in health and disease — Minireview. Eur J Microbiol Immunol. (Bp), 2: 97–102. https://doi.org/10.1556/eujmi.2.2012.2.1.

[28] Hossain, T.J. (2024). Methods for screening and evaluation of antimicrobial activity: A review of protocols, advantages, and limitations. Eur J Microbiol Immunol. (Bp), 14: 97–115. https://doi.org/10.1556/1886.2024.00035.